Mechanical and thermal expansion properties of aligned carbon nanotube reinforced epoxy composites

doi: 10.1299/mej.19-00012

Bulletin of the JSME Vol.0, No.0, 2017
Mechanical Engineering Journal

Mechanical and thermal expansion properties of aligned carbon nanotube reinforced epoxy composites

Keiichi SHIRASU*, Itaru TAMAKI*, Go YAMAMOTO** and Toshiyuki HASHIDA*
* Fracture and Reliability Research Institute, Tohoku University
6-6-11, Aramaki Aoba, Aobaku, Sendai, Miyagi 980-8579, Japan
E-mail: keiichi.shirasu@rift.mech.tohoku.ac.jp
** Department of Aerospace Engineering, Tohoku University
6-6-01, Aramaki Aoba, Aobaku, Sendai, Miyagi, 980-8579 Japan

Received 30 October 2017

Abstract
Aligned MWCNT/epoxy composites made with the three types of the multi-walled carbon nanotubes (MWCNTs) with different thermal annealing temperature have been prepared, and the tensile tests and thermal expansion tests of the composites in the MWCNT alignment direction were conducted to evaluate the effects of crystallinity of MWCNTs on the mechanical and thermal expansion properties of aligned MWCNT reinforced epoxy composites. Additionally, the coefficients of thermal expansion (CTEs) of the MWCNTs in the axial direction were computed by using the Young's modulus of the MWCNTs and the CTE of the composites in Turner's model. The annealing temperatures of the MWCNTs were 2400˚C and 2900˚C. It was shown that the thermal annealing of MWCNTs was effective for improving the crystallinity of the MWCNTs, while it had no major effects on both tensile strength and Young's modulus of the composites. This is mainly because the thermally annealed MWCNTs themselves possessed almost comparable nominal tensile strength (~4–5 GPa) and Young's modulus (~200 GPa) compared with the as-grown MWCNTs. On the other hand, we demonstrated by thermal expansion testing that the thermal contraction of the composites in the nanotube alignment direction was observed by the addition of MWCNTs. All the MWCNTs possessed negative CTEs and the CTEs tend to become more negative with increasing annealing temperature. This is probably because of a decrease in the number of small defects (vacancies and Stone-Wales defects) and intershell cross-linking defects associated with sp^3 carbons, and an increase in the sp^2 carbons owing to the high-temperature thermal annealing.

Key words :Carbon nanotubes, Polymer materials, Composites, Coefficient of thermal expansion, Crystallinity

1. Introduction

Recently, twist-spun yarns and continuous unidirectional sheets comprising multi-walled carbon nanotube (MWCNT), which are fabricated by directly drawing MWCNTs from drawable MWCNT forests, have been developed (Jiang, et al., 2002; Zhang, et al., 2004, 2005), and novel processing methods utilizing twist-spun yarns and unidirectional sheets have emerged as means of producing composites and electronic devices. To make decisions on fundamental design of composites and devices, the understanding the coefficient of thermal expansion (CTE) as well as the mechanical properties of CNTs is essential. In particular, electronic devices may experience high temperatures during manufacture and operation processes, which lead to differential thermal expansion and residual stresses in devices, and affects the device reliability. Many experimental studies to date have focused on a CTE of MWCNTs in the radial direction and its temperature dependence (Bandow, 1997; Maniwa, et al., 2001a, 2001b). However, experimental studies for an axial CTE of CNTs are quite limited, and instead thermal expansion behaviors of composites reinforced with CNTs were evaluated. For example, Alamusi et al. (2013) evaluated the thermal expansion

Paper No.xx-xxxx
[DOI: 10.1299/xxx.2014xxx000x]

properties of CNT/epoxy composites using a multi-scale numerical technique in which the effects of both CNT weight fraction and temperature were investigated. The numerical results were in reasonable agreement with the values obtained from both the experimental and theoretical results. Deng, et al. (2014) studied the CTEs of single-walled CNTs (SWCNTs) and double-walled CNTs (DWCNTs) by measuring the dependence of Raman spectroscopy of nanotubes in epoxy composites. The CTE values of both SWCNTs and DWCNTs were determined to be positive, however, the CTEs in the radial direction as well as those in the axial direction may affect the experimental results due to a random distribution of the CNTs in the epoxy matrix. Some researchers also investigated analytically the temperature dependence of axial CTEs of CNTs (Raravikar, et al., 2002; Schelling and Keblinski, 2003; Kwon, et al., 2004; Jiang, et al., 2004; Alamusi, et al., 2012). Recently, the authors investigated experimentally the thermal expansion behavior of aligned MWCNT/epoxy composites in the direction of MWCNT alignment, and the CTE of the MWCNTs in the axial direction were deduced by Turner's model (Shirasu, et al., 2015). We demonstrated that the negative thermal expansion observed in the composites increased with a volume fraction of MWCNTs, and the axial CTE of the investigated MWCNTs with an average outer diameter of 40 nm estimated to be negative. In addition to above study, we evaluated the CTE of MWCNTs with smaller outer diameter (average 25 nm) but comparable inner diameter and crystallinity compared with the MWCNTs with average outer diameter of 40 nm, and showed that the MWCNTs with average outer diameter of 40 nm possessed larger negative CTE than that with average outer diameter of 25 nm (Shirasu, et al., 2016, 2017a).

It is well known that CNTs and graphene with sp^2 hybridized bonds has negative CTE (Bailey and Yates, 1970). This negative CTE can be explained by Grüneisen theory, i.e., whether a solid expands or contracts upon heating depends on the balance between phonon modes with positive and negative Grüneisen parameters (Schelling and Keblinski, 2003). At low temperatures, transverse acoustic modes which correspond to the out-of-plane atomic vibrations of the crystal lattice may exhibit negative Grüneisen parameters. Schelling and Keblinski (2003) investigated the thermal expansion property of SWCNTs using both lattice dynamics calculations and molecular dynamics (MD) simulations. They found that the axial CTE of SWCNTs at room temperature was negative while it showed positive at high temperatures. The results obtained our previous studies as mentioned above may be explained by the Grüneisen theory. However, the structure and crystallinity of the experimentally grown CNTs vary with synthesis method and conditions, and normally such CNTs possess structural defects composed of sp^3 bonds. Diamond which is composed of sp^3 hybridized carbon atoms shows positive CTE. In fact, Schelling and Keblinski (2003) demonstrated that the diamond showed the positive Grüneisen parameters, resulting in positive value of CTE at all temperatures. Thus, the CTE of CNTs may depend on the crystallinity (i.e. the amount of sp^3 carbons). Furthermore, the crystallinity of CNTs may affect the mechanical properties of CNTs itself and CNT reinforced composites as well as the CTE. Because precise knowledge of the CTE and mechanical properties of experimentally grown MWCNTs with different crystallinity are crucial in designing CNT-based composites and devices, the evaluation of effects of crystallinity of MWCNTs are needed.

Here, we investigated the effects of annealing temperature of MWCNTs on the mechanical and thermal expansion properties of composites. It is well known that the thermal annealing is effective for improving the crystallinity of MWCNTs. As-grown MWCNTs and two types of thermally annealed MWCNTs with annealing temperature of 2400˚C and 2900˚C were prepared, and these MWCNTs possess a significantly different crystallinity but with almost the same diameter and length. To determine the CTE of MWCNTs in the axial direction, the CTE of composites in the MWCNT alignment direction was evaluated and the axial CTE of the MWCNTs was estimated using the Turner's model.

2. Experimental procedure

Drawable MWCNT forests were synthesized by a chloride mediated chemical vapor deposition method using acetylene and iron (II) chloride as the base material and the catalyst, respectively. The detailed procedure for the preparation of drawable MWCNT forests is reported elsewhere (Inoue, et al., 2008). The outer diameter, inner diameter and length of the MWCNTs were approximately 40 nm, 8 nm and 700 μm, respectively. The MWCNT sheets were dry-drawn from the drawable MWCNT forests and wound onto a rotating plate (Shirasu, et al., 2017c), and then thermally-annealed by using a resistance heated graphite element furnace (Kurata Giken SCC-U-80/150, Japan) under argon atmosphere. Annealing temperatures are 2400˚C and 2900˚C. The outer diameter, inner diameter and the number of nanotube shells of the MWCNTs are summarized in Table 1. Transmission electron microscopy (TEM; JEOL

[DOI: 10.1299/xxx.2014xxx000x]

Table 1 Outer diameter, inner diameter and the number of nanotube shells for three types of MWCNTs. The MWCNTs used in this study possessed almost the same outer and inner diameter.

Annealing temperature (˚C)	Outer diameter (nm)	Inner diameter (nm)	The number of nanaotube shells
As-grown	40 ± 10	8 ± 3	47 ± 12
2400	36 ± 9	7 ± 2	43 ± 13
2900	41 ± 11	7 ± 2	50 ± 15

JEM-2100F, Japan) observation showed that the MWCNTs have almost the same outer and inner diameter. Raman scattering spectroscopy (JASCO NRS-5100, Japan) was used to measure the nanotube crystallinity, and the Raman intensity ratios ($R = I_D/I_G$) were calculated for each sample, along with the average and standard deviation for each of the MWCNT type. The measurements were carried out at room temperature under ambient conditions using an argon ion laser with an excitation wavelength of 532 nm.

Aligned MWCNT reinforced epoxy composites were fabricated by a hot-melt prepreg method (Ogasawara, et al., 2011). The MWCNT monolithic sheets and a partially cured epoxy resin (B-stage epoxy) with a release paper were used as the starting materials. The epoxy resin system was bisphenol-A type epoxy, novolac-type epoxy, and an aromatic diamine hardener. The detailed procedure for composite preparation is described elsewhere (Shirasu, et al., 2017a). We calculated the weight fraction of MWCNTs from the masses of the MWCNT sheets (before impregnation of the epoxy) and the composites. Having obtained the weight fraction of the MWCNTs, we calculated the volume fraction of MWCNTs assuming that the densities of the MWCNTs and epoxy were 2.0 g/cm^3 and 1.2 g/cm^3, respectively. The volume fraction of MWCNTs was controlled by changing the number of wound layers of MWCNT sheets, and the values for the composite samples prepared were found to be in the range from 15 to 26 vol.%.

Tensile tests of the composites in the MWCNT alignment direction were conducted to evaluate the tensile strength, Young's modulus and failure strain using a tensile test apparatus (Instron Model 5965, USA) with a 50 N load cell. The length, width and thickness of the samples were 45 mm, 2 mm and 0.030–0.040 mm, respectively, where the length is along the MWCNT alignment direction. The width and thickness dimensions of the composite samples were measured by the scanning electron microscope (SEM; JEOL JSM6510, Japan). The crosshead speed was 0.2 mm/min and the gauge length was approximately 18 mm. Strain was measured by a laser displacement meter with a resolution of 0.1 μm (Keyence LS-7600, Japan), following which the Young's modulus was calculated from the slope of the stress-strain curve.

We measured the CTE of the composites in the MWCNT alignment direction. The detailed procedure for CTE measurement has been reported elsewhere (Shirasu, et al., 2017a). The sample was put on a temperature control unit (a Peltier cooling stage and a hot plate), and the temperature of the composite sample was measured by a thermocouple. The length change was monitored by a laser displacement meter in the temperature range from 0 to 40˚C. The ramping rate was 10 K/min. In this study, the average CTE of the composites in the above temperature range was evaluated, and the formula of CTE is given:

$$\alpha_c = \frac{\Delta L/L}{\Delta T} \tag{1}$$

where α_c is the CTE of the composites, ΔT is the temperature difference (40 K), L is the initial length of the sample and ΔL is the increased length. The slope of $\Delta L/L$ against ΔT curve over the temperature range was obtained using experimental data to determine α_c. The CTEs of the MWCNTs were calculated by substituting the CTE of the epoxy and composites and Young's modulus of the epoxy and MWCNTs into Turner's model (Turner, 1934) such that:

$$\alpha_c = \frac{\alpha_m(1-V_{CNT})E_m + \alpha_{CNT}V_{CNT}E_{CNT}}{(1-V_{CNT})E_m + V_{CNT}E_{CNT}} \tag{2}$$

where V is the volume fraction and α and E are the CTE and Young's modulus. The subscripts "CNT" and "m" for V, E and α refer to the CNT and matrix, respectively. The CTEs of the MWCNTs (α_{CNT}) were calculated for each specimen, along with the average and standard deviation for each of the MWCNT type.

[DOI: 10.1299/xxx.2014xxx000x]

3. Results and discussion

First, TEM and Raman spectroscopic technique were used to evaluate whether the structural evolution is occurring during annealing process. Fig. 1 shows TEM images and Raman intensity ratio ($R = I_D/I_G$) of the MWCNTs. It can be seen that the R values decrease with the increasing annealing temperature, which suggests that the defective structure transformed into a stable graphite planer structure by the annealing treatment. This structural evolution can be also observed by TEM. The as-grown MWCNTs consist of slightly undulating graphitic hollow structure with the nanotube axis (Fig. 1a), and they possess several types of structural defects such as *discontinuous flaws*, *kinks and bends* and *remnant catalysts* (Fig. 1a, b). For the nanotubes annealed at 2400˚C (Fig. 1c), the degree of waviness of the nanotube shells seems to decrease. Through the thermal annealing at 2900˚C (Fig. 1d), the undulating structure disappears and the MWCNT consists of nested graphitic multiwalled shells that are almost perfectly aligned with the nanotube axis, even though the structural defects such as *kinks and bends* were still visible on a subset of the nanotubes (Fig. 1e).

Figure 2 shows the cross-sectional views of the composite and the MWCNT distribution in the composite as observed by SEM. The epoxy resin well penetrated between MWCNTs and the majority of the MWCNTs are aligned although some MWCNTs are inclined with respect to the alignment direction. Tensile tests were carried out on the aligned MWCNT reinforced epoxy composites to evaluate the mechanical properties. Fig. 3 shows the Young's moduli, tensile strengths and failure strains of the composites. The Young's moduli and tensile strengths of the composites tend to increase with the MWCNT volume fraction regardless of the annealing temperature. However, the thermal annealing has no major effects on both properties. Additionally, no significant annealing temperature and MWCNT volume fraction dependence of failure strain is seen, and its value is approximately 0.5%. The authors have investigated experimentally the mechanical properties of the individual MWCNTs by conducting uniaxial tensile tests that have been performed with a manipulator inside the vacuum chamber of SEM. The detailed procedure for tensile testing is described elsewhere (Yamamoto, et al., 2010; Shirasu, et al., 2017b). The measured mechanical properties including nominal tensile strength, Young's modulus and failure strain are summarized in Table 2. It can be seen that no clear difference in the mechanical properties between as-grown and thermally annealed MWCNTs is seen, which suggests that the structural changes observed in this annealing conditions used in this study may lead to no significant effect on both the nominal tensile strength and Young's modulus. This is mainly because the as-grown MWCNTs used in this study include the structural defects, i.e., *kinks and bends* and *discontinuous flaws* that are not completely removed by thermal annealing and are still observed in the thermally annealed MWCNTs even though the as-grown MWCNTs possess an intermediate level of crystallinity ($R = 0.31$) (Shirasu, et al., 2017b).

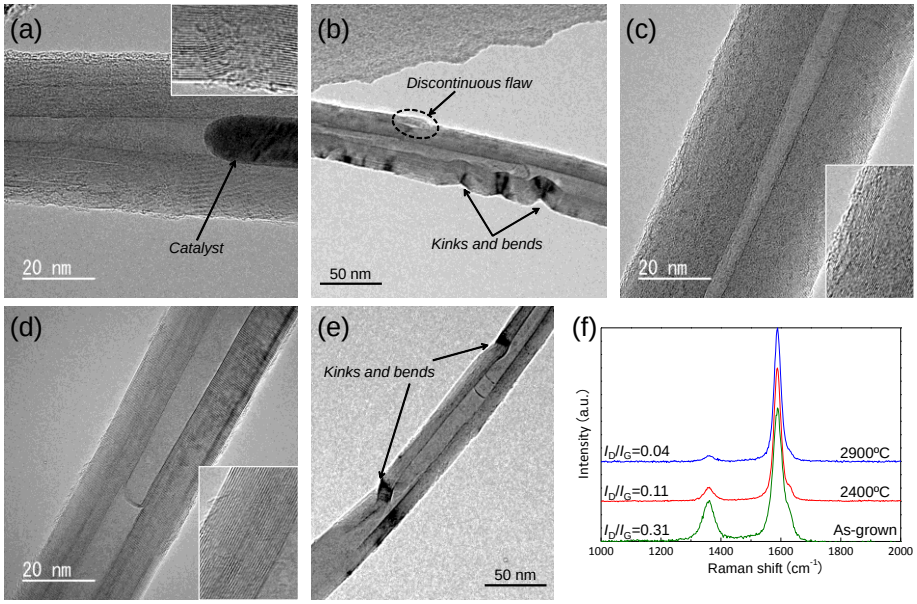

Fig. 1 TEM images of the (a, b) as-grown MWCNTs and thermally-annealed MWCNTs at (c) 2400˚C and (d, e) 2900˚C. (f) Raman spectra of three types of MWCNTs. Arrows indicate the position of *discontinuous flaw*, *kinks and bends* and *remnant catalyst*. Through the thermal annealing, the undulating graphitic hollow structure transformed into a stable graphite planer structure, and the Raman intensity ratio ($R = I_D/I_G$) decreased with increasing annealing temperature.

[DOI: 10.1299/xxx.2014xxx000x]

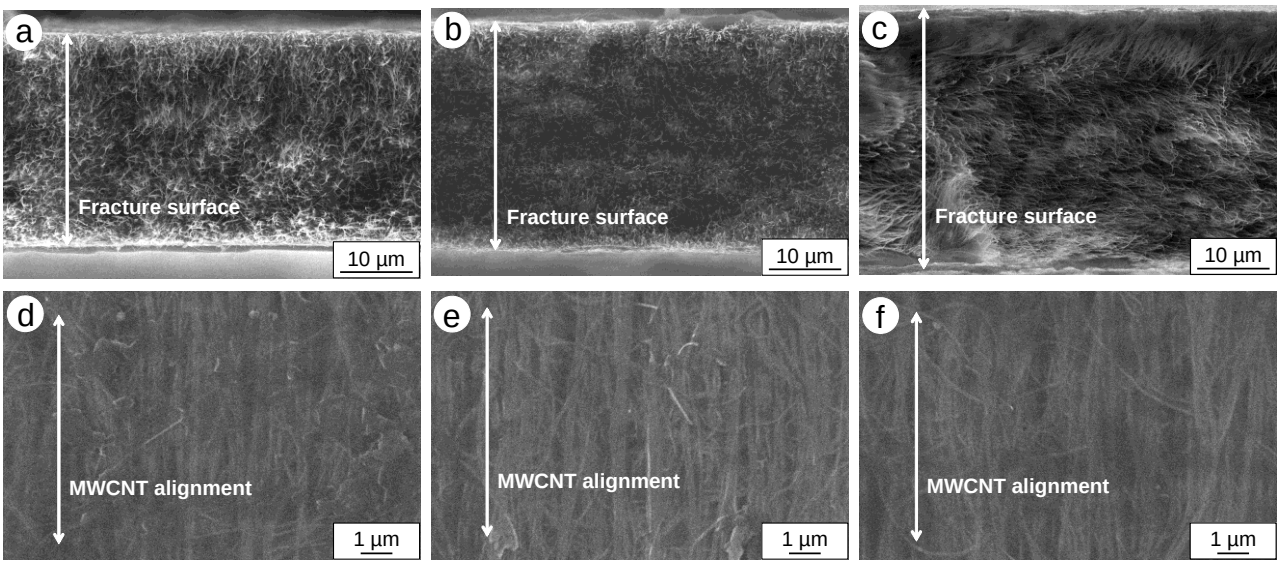

Fig. 2 SEM images of the composites containing (a, d) as-grown MWCNTs, (b, e) MWCNTs annealed at 2400˚C and (c, f) MWCNTs annealed at 2900˚C showing (a, b, c) the cross-section and (d, e, f) in-plane MWCNT distribution in the composites. The epoxy resin well penetrated between MWCNTs and the majority of the MWCNTs were aligned although some MWCNTs were inclined with respect to the alignment direction.

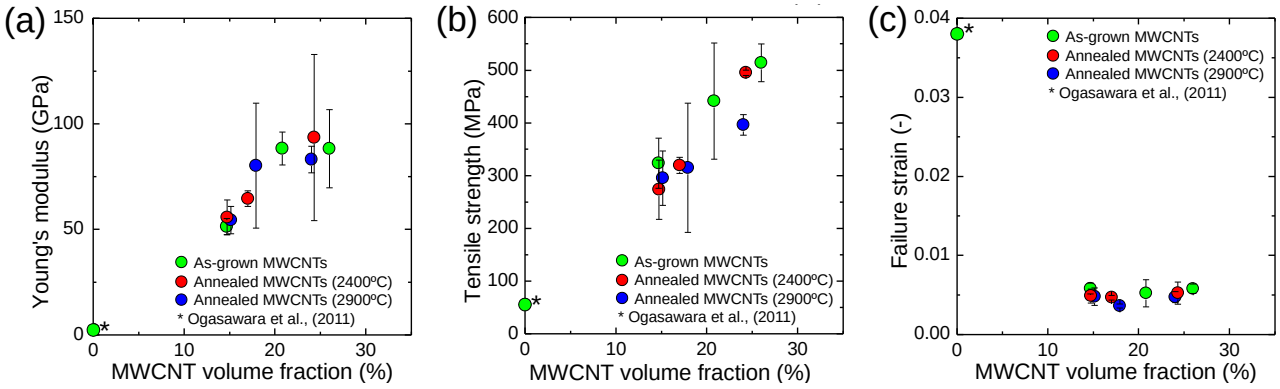

Fig. 3 (a) Young's modulus, (b) tensile strength and (c) failure strain of the composites containing three types of MWCNTs. Although the Young's moduli and tensile strengths of the composites increased with the MWCNT volume fraction regardless of the annealing temperature, the thermal annealing had no major effects on both properties.

Table 2 Nominal tensile strength, Young's modulus and failure strain for three types of MWCNTs.

Annealing temperature (˚C)	Nominal tensile strength (GPa)	Young's modulus (GPa)	Failure strain (%)
As-grown[a]	5.2 ± 2.1	210 ± 143	3.0 ± 0.6
2400	4.9 ± 1.2	214 ± 60	2.4 ± 0.3
2900[a]	3.8 ± 1.5	227 ± 103	2.0 ± 0.4

[a]: Shirasu, et al., (2017b)

Next, the thermal expansion property of the aligned MWCNT reinforced epoxy composites was evaluated. The variations of the thermal strain of the pure epoxy and composites in the MWCNT alignment direction as a function of temperature difference are shown in Fig. 4. The thermal strain of the epoxy increases with the temperature. However, the thermal strain of the composites containing as-grown MWCNTs significantly decreases with the addition of 16 vol.% MWCNTs, and thermal contraction is seen in composites containing 21 vol.% MWCNTs. The composites containing thermally-annealed MWCNTs show that a trend of decreasing thermal strain is observed with the increasing temperature regardless of the volume fraction of MWCNTs. These results suggest that the MWCNTs have negative

[DOI: 10.1299/xxx.2014xxx000x]

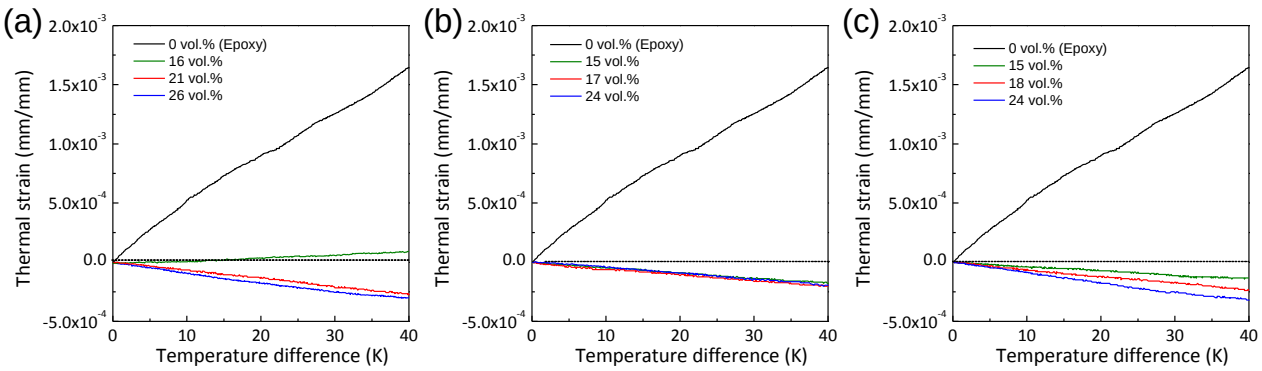

Fig. 4 Thermal strain of composites containing (a) as-grown MWCNTs, (b) thermally-annealed MWCNTs at 2400˚C and (c) thermally-annealed MWCNTs at 2900˚C as a function of temperature difference. The thermal strain of the composites significantly decreased by the addition of MWCNTs and the negative thermal expansion was observed in the composites containing large volume fraction of MWCNTs.

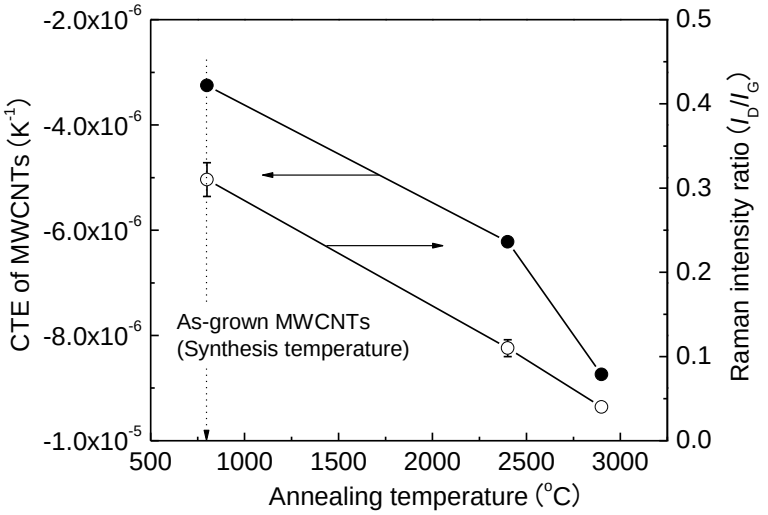

Fig. 5 CTE of the MWCNTs and Raman intensity ratio as a function of annealing temperature of MWCNTs. The MWCNTs possessed negative CTEs and the CTEs became more negative with increasing annealing temperature, and the CTE was correlated with the Raman intensity ratio.

axial CTE values. The MWCNTs possessed a high aspect ratio (length/diameter > 17000) and were aligned along almost the same direction in the composites. Thus, the composites can be modeled as polymer composites reinforced with unidirectionally aligned fibers, and the CTE of the composites in the MWCNT alignment direction, α_c, may be expressed by Turner's model (Turner, 1934) as described in Eq. (2). The Young's moduli of the MWCNTs used in this study are listed in Table 2. The CTE and Young's modulus of the epoxy are 3.9×10^{-5} K^{-1} and 2.5 GPa (Ogasawara, et al., 2011), respectively. Fig. 5 shows the dependence of the CTE of the MWCNTs upon the annealing temperature of the MWCNTs. In addition to the CTE dependence, Fig. 5 gives the relationship between Raman intensity ratio and annealing temperature. The MWCNTs possess negative CTEs and the CTEs tend to become more negative with increasing annealing temperature, and the CTE is correlated with the Raman intensity ratio. Here, the authors have discussed the effect of MWCNT orientation on the CTE of the composites in the MWCNT alignment direction (Shirasu, et al., 2016). Even though the composites prepared by the same method in this study had the orientation factor of 0.8 (for a perfectly aligned sample, the orientation factor would be 1 and for a composite where the MWCNTs are randomly oriented, the orientation factor would be 0), we confirmed that this degree of mis-alignment is so small that this inclination is negligible within the required calculation accuracy. As mentioned in the Introduction, it is well known that diamond which is composed of sp^3 hybridized carbon atoms shows positive CTE, while graphene with sp^2 hybridized bonds has negative CTE (Bailey and Yates, 1970). Schelling and Keblinski (2003) studied that the axial CTE for the SWCNTs was -0.9×10^{-6} K^{-1} at room temperature, and this result was associated with the negative

[DOI: 10.1299/xxx.2014xxx000x]

Grüneisen parameters. On the other hand, for the diamond, all the Grüneisen parameters were positive, which led to a positive CTE at all temperatures. Demichelis et al. (1993) evaluated the CTE of hydrogenated amorphous carbon films with different concentrations of sp^2 carbon. These researchers showed that CTE of the hydrogenated amorphous carbon films varied with the sp^2/sp^3 ratio. Emmerich (2014) showed the axial CTE of several kinds of polyacrylonitrile (PAN)-based carbon fibers (Torayca® T1000, M40J and M60J) manufactured by Toray Industries, Inc. The axial CTE of such carbon fibers at room temperature were in the range of $-1.10 - -0.55 \times 10^{-6}$ K^{-1} whose absolute values are smaller than those of MWCNTs used in this study. This discrepancy may be due to the irregular arrangement of the graphene layers in the carbon fibers. Nonetheless, it depended on the fiber crystallinity, i.e., the negative CTE increased with decreasing longitudinal concentration of defective region of length and increasing Young's modulus and electrical conductivity. In addition to above studies, we have evaluated the axial CTE of DWCNTs with different number of defects such as vacancy and sp^3 intershell crosslinks by MD simulations, which demonstrated that the DWCNTs with smaller amount of defects were shown to possess negative CTEs, but the CTEs tended to become less negative or positive values with increasing the number of defects (unpublished data). The as-grown MWCNTs used in this study showed higher intensity of D-band compared with the thermally annealed MWCNTs, suggesting that the as-grown MWCNTs had a large amount of small defects (i.e., vacancies, Stone-Wales defects and intershell cross-linking defects associated with sp^3 carbons) in addition to the structural defects as shown in Fig. 1a and b. These small defects and sp^3 carbons may cause reduction of the negative CTE of the MWCNT in the axial direction. On the other hand, when the MWCNTs were annealed at 2900˚C, its crystallinity considerably increased (R = 0.04). This can be explained by a decrease in the number of such small defects and intershell cross-linking defects, and an increase in the sp^2 carbons owing to the high-temperature annealing, resulting in increasing the negative CTE.

4. Conclusions

In this study, aligned MWCNT/epoxy composites made with the three types of the MWCNTs with different thermal annealing temperature have been prepared, and the mechanical and thermal expansion properties of the composites in the MWCNT alignment direction were investigated. It was shown that the thermal annealing of MWCNTs is effective for improving the MWCNTs' crystallinity and the Raman intensity ratio (I_D/I_G) decreased from 0.31 to 0.04. However, it had no major effects on both tensile strength and Young's modulus of the composites, which is mainly because there is no apparent difference in the mechanical properties of MWCNT itself between as-grown and thermally annealed MWCNTs. On the other hand, thermal expansion tests demonstrated that the thermal strain of the composites significantly decreased by the addition of MWCNTs and the negative thermal expansion was observed in the composites containing large volume fraction of MWCNTs. Based on these results, the CTEs of the MWCNT in the axial direction were estimated by using the CTE of the composites and the Young's modulus of the MWCNTs in Turner's model. The MWCNTs possessed negative CTEs and the CTEs tended to become more negative with the increment of the annealing temperature. This is likely to be because a decrease in the number of small defects (vacancies, Stone-Wales defects) and intershell cross-linking defects associated with sp^3 carbons, and an increase in the sp^2 carbons owing to the high-temperature thermal annealing.

Acknowledgement

The authors thank Toyo Tanso Co., Ltd. for its technical assistance in thermal annealing of the MWCNTs. The authors acknowledge Dr. T. Miyazaki of the Technical Division, School of Engineering, Tohoku University, for technical assistance in the TEM analysis. This research was partially supported by the Grant-in-Aid for Young Scientists (B) 16K20904, the Grant-in-Aid for Young Scientists (A) 15H05502.

References

Alamusi, Hu, N., Jia, B., Arai, M., Yan, C., Li, J., Liu, Y., Atobe, S. and Fukunaga, H., Prediction of thermal expansion properties of carbon nanotubes using molecular dynamics simulations, Computational Materials Science, Vol.54 (2012), pp.249–254.

Alamusi, Hu, N., Qiu, J., Li, Y., Chang, C., Atobe, S., Fukunaga, H., Liu, Y., Ning, H., Wu, L., Li, J., Yuan, W.,

Watanabe, T., Yan, C. and Zhang, Y., Multi-scale numerical simulations of thermal expansion properties of CNT-reinforced nanocomposites, Nanoscale Research Letters, Vol.8, No.15 (2013). http://www.nanoscalereslett.com/content/8/1/15

Bailey, A.C. and Yates, B., Anisotropic thermal expansion of pyrolytic graphite at low temperatures, Journal of Applied Physics, Vol.41, No.13 (1970), pp.5088-5091.

Bandow, S., Radial thermal expansion of purified multiwall carbon nanotubes measured by X-ray diffraction, Japanese Journal of Applied Physics, Vol.36, No.108 (1997), pp. L1403-L1405.

Demichelis, F., Pirri, C. F., Tagliaferro, A., Benedetto, G., Boarino, L., Spagnolo, R., Dunlop, E., Haupt, J. and Gissler, W., Mechanical and thermophysical properties of diamond-like carbon (DLC) films with different sp^3/sp^2 ratios, Diamond & Related Materials, Vol.2, No.5-7 (1993), pp.890-892.

Deng, L., Young, R.J., Kinloch, I.A., Sun, R., Zhang, G., Noé, L. and Monthioux. M., Coefficient of thermal expansion of carbon nanotubes measured by Raman spectroscopy, Applied Physics Letters, Vol.104 (2014), Article No.51907.

Emmerich, F.G., Young's modulus, thermal conductivity, electrical resistivity and coefficient of thermal expansion of mesophase pitch-based carbon fibers, Carbon, Vol. 79 (2014), pp.274–293.

Inoue, Y., Kakihata, K., Hirono, Y., Horie, T., Ishida, A. and Miura, H., One-step grown aligned bulk carbon nanotubes by chloride mediated chemical vapor deposition, Applied Physics Letters, Vol.92, No.21 (2008), Article No.213113.

Inoue Y, Suzuki Y, Minami Y, Muramatsu J, Shimamura Y, Suzuki K, Ghemes, A., Okada, M., Sakakibara, S., Mimura, H. and Naito, K., Anisotropic carbon nanotube papers fabricated from multiwalled carbon nanotube webs, Carbon, Vol. 49, (2011), pp. 2437–2443.

Jiang, H., Liu, B., Huang, Y. and Hwang, K. C., Thermal expansion of single wall carbon nanotubes, Journal of Engineering Materials and Technology, Vol.126, No.3 (2004), pp.265–270.

Kwon, Y. K., Berber, S. and Tománek, D., Thermal contraction of carbon fullerene and nanotubes, Physical Review Letters, Vol.92, No.1 (2004), Article No.015901.

Maniwa, Y., Fujiwara, R., Kira, H., Tou, H., Nishibori, E., Takata, M., Sakata, M., Fujiwara, A., Zhao, X., Iijima, S. and Ando, Y., Multiwalled carbon nanotubes grown in hydrogen atmosphere: An x-ray diffraction study, Physical Review B, Vol.64, No.7 (2001a), Article No.073105.

Maniwa, Y., Fujiwara, R., Kira, H., Tou, H., Kataura, H., Suzuki, S., Achiba, Y., Nishibori, E., Takata, M., Sakata, M., Fujiwara, A. and Suematsu, H., Thermal expansion of single-walled carbon nanotube (SWNT) bundles: X-ray diffraction studies, Physical Review B, Vol.64, No.24 (2001b), Article No.241402(R).

Ogasawara, T., Moon, S. Y., Inoue, Y. and Shimamura, Y., Mechanical properties of aligned multi-walled carbon nanotube/epoxy composites processed using a hot-melt prepreg method, Composites Science and Technology, Vol.71, No.16 (2011), pp.1826–1833.

Raravikar, N. R., Keblinski, P., Rao, A. M., Dresselhaus, M. S., Schadler, L. S. and Ajayan, P. M., Temperature dependence of radial breathing mode Raman frequency of single-walled carbon nanotubes, Physical Review B, Vol.66, No.23 (2002), Article No.235424.

Schelling, P. K. and Keblinski, P., Thermal expansion of carbon structures, Physical Review B, Vol.68, No.3 (2003), Article No.035425.

Shirasu, K., Yamamoto, G., Tamaki, I., Ogasawara, T., Shimamura, Y., Inoue, Y. and Hashida, T., Negative axial thermal expansion coefficient of carbon nanotubes: Experimental determination based on measurements of coefficient of thermal expansion for aligned carbon nanotube reinforced epoxy composites, Carbon, Vol.95 (2015), pp.904–909.

Shirasu, K., Nakamura, A., Yamamoto, G., Ogasawara, T., Shimamura, Y., Inoue, Y. and Hashida, T., Temperature dependence of axial thermal expansion coefficient of multi-walled carbon nanotubes (A procedure based on measurements of coefficient of thermal expansion for aligned carbon nanotube/epoxy composites), Transactions of the JSME (in Japanese), Vol.82, No.844 (2016), Article No.16-00228.

Shirasu, K., Nakamura, A, Yamamoto, G., Ogasawara, T., Shimamura, Y., Inoue, Y. and Hashida, T., Potential use of CNTs for production of zero thermal expansion coefficient composite materials: An experimental evaluation of axial thermal expansion coefficient of CNTs using a combination of thermal expansion and uniaxial tensile tests, Composites Part A: Applied Science and Manufacturing, Vol.95 (2017a), pp.152-160.

[DOI: 10.1299/xxx.2014xxx000x]

Shirasu, K., Tamaki, I, Miyazaki, T., Yamamoto G, Bekarevich, R., Hirahara, K, Shimamura, Y., Inoue, Y. and Hashida, T., Key factors limiting carbon nanotube strength: Structural characterization and mechanical properties of multi-walled carbon nanotubes, Mechanical Engineering Journal, Vol.4, No.5 (2017b) Article No.17-00029.

Shirasu, K., Yamamoto, G., Inoue, Y., Ogasawara, T., Shimamura, Y. and Hashida, T., Development of large-movements and high-force electrothermal bimorph actuators based on aligned carbon nanotube reinforced epoxy composites, Sensors and Actuators A: Physical, Vol.267 (2017c), pp.455-463.

Turner, P.S., Thermal-expansion stresses in reinforced plastics, Journal of Research of the National Bureau of Standards, Vol.37 (1946), pp.239-250.

Yamamoto, G, Suk, J.W., An, J., Piner, R.D., Hashida, T., Takagi, T. and Ruoff, R.S., The influence of nanoscale defects on the fracture of multi-walled carbon nanotubes under tensile loading, Diamond & Related Materials, Vol.19 No.7-9 (2010), pp.748–751.

Zhang, M., Atkinson, K. R. and Baughman R. H., Multifunctional carbon nanotube yarns by downsizing an ancient technology, Science, Vol.306, No.5700 (2004), pp.1358-1361.

Zhang, M., Fang, S., Zakhidov, A. A., Lee, S. B., Aliev, A. E., Williams, C. D., Atkinson, K. R. and Baughman, R. H., Strong, transparent, multifunctional, carbon nanotube sheets, Science, Vol.309, No.5738 (2005), pp.1215–1219.

[DOI: 10.1299/xxx.2014xxx000x]